In Vivo Kinematics of the Knee during Weight Bearing in High Flexion

Wei Qi[1,2], **Ali Hosseini**[1], **Tsung-Yuan Tsai**[1], **Jing-Sheng Li**[1], **Harry E. Rubash**[1], and **Guoan Li**[1,*]

[1]Bioengineering Laboratory, Department of Orthopaedic Surgery, Massachusetts General Hospital/Harvard Medical School, 55 Fruit Street, GRJ 1215, Boston, MA 02114, United States

[2]Department of Orthopaedic Surgery, Chinese PLA General Hospital, 28 Fuxing Road, Beijing 100853, P.R. China

Abstract

Achieving high flexion is an objective of contemporary total knee arthoplasty, however little is known on the knee biomechanics at high flexion under weight-bearing conditions. This study is to investigate the 6DOF kinematics and tibiofemoral cartilage contact biomechanics of the knee during weight-bearing flexion from full extension to maximal flexion. Eight knees from seven healthy subjects with no history of injuries or chronic pain were recruited. The knees were MRI scanned to create 3D models of the tibia and femur, including their articular cartilage surfaces. The subjects were then imaged using a dual fluoroscopic image system while performing a weight-bearing quasi-static single-legged lunge from full extension to maximal flexion. The 6DOF kinematics and the articular cartilage contact locations were measured along the flexion path of the knee. The result indicated that the internal tibial rotation increased sharply at low flexion angles (full extension to 30°), maintained a small variation in the middle range of flexion (30° to 120°), and then sharply increased again at high flexion angles (120° to maximal flexion). The contact point moved similarly in the medial and lateral compartments before 120° of flexion, but less on the medial compartment at high flexion angles. The results indicated that the knee motion couldn't be described using one character in the entire range of flexion, especially in high flexion. The knee kinematic data in the entire range of flexion of the knee could be instrumental for designing new knee prostheses to achieve physical high flexion and improving rehabilitation protocols after knee injuries.

Keywords

In vivo knee kinematics; Cartilage contact; High flexion

Corresponding Author: Guoan Li, Bioengineering Laboratory, 55 Fruit Street, GRJ 1215, Boston, MA 02114, **Telephone**: 1-617-726-1346, **Fax**: 1-617-724-4392, GLI1@PARTNERS.ORG.

Publisher's Disclaimer: This is a PDF file of an unedited manuscript that has been accepted for publication. As a service to our customers we are providing this early version of the manuscript. The manuscript will undergo copyediting, typesetting, and review of the resulting proof before it is published in its final citable form. Please note that during the production process errors may be discovered which could affect the content, and all legal disclaimers that apply to the journal pertain.

Conflict of interest statement
We declare that there are no issues that may be considered as potential conflicts of interest to this work.

1. Introduction

Investigation of characteristic motion of the knee is critical for design and evaluation of contemporary total knee arthroplasty (TKA) that aims to restore normal knee function and achieve full range of knee flexion (Fitz et al., 2012; Kuroyanagi et al., 2012; Moynihan et al., 2010; Tamaki et al., 2009). Medial-pivoting motion during knee flexion, that describes the knee rotation along an axis located at the medial side of the knee during flexion, has been widely accepted as a motion character and has been implemented in several current TKA components such as Advance (Wright Medical Technology, Arlington, TN) and Journey (Smith & Nephew Inc., Memphis, TN) (Fitz et al., 2012; Kuroyanagi et al., 2012; Moynihan et al., 2010). While many studies have reported data to support the medial-pivoting feature of the knee motion (Hill et al., 2000; Jensen, 2005; Johal et al., 2005; Tanifuji et al., 2011), there are studies that reported knee flexion in a lateral-pivoting pattern during gait (Hoshino and Tashman, 2012; Koo and Andriacchi, 2008; Kozanek et al., 2009). Recently, several studies also have reported various motion patterns of the knee, implying that the motion characters are activity (or loading) dependent (Acker et al., 2011; Amin et al., 2008; Hoshino and Tashman, 2012; Johal et al., 2005; Palmer, 2012).

Several studies on knee motion have used various methods to measure the knee kinematics. To use the magnetic resonance (MR) imaging methods, two sagittal plane images are usually selected from the medial and lateral compartments at each flexion angle to analyze the articular cartilage contact locations (Johal et al., 2005). Single plane fluoroscopic images are also widely used to investigate knee motion where 3D knee joint models are matched to the images captured at each knee flexion angle (Tanifuji et al., 2011). Traditional motion analysis methods use digital cameras to capture the motion of the reflective markers fixed on the skin (Gao and Zheng, 2008; Koo et al., 2011). Bi-plane radiographic image methods match the 3D knee joint models to the two images captured simultaneously from two directions at each flexion angle (Anderst and Tashman, 2003; Kozanek et al., 2009). Despite these various studies, the kinematic features of the knee along the weight-bearing flexion path from full extension (FE) to maximal flexion, especially the knee kinematics in high flexion angles, have not been accurately investigated. This knowledge could be an important reference for improvement of contemporary TKA surgeries that aim to restore full range of knee flexion.

The objective of this study is to investigate the 6 degrees of freedom (DOF) kinematics of the knee and the tibiofemoral articular cartilage contact biomechanics during weight-bearing flexion from full extension to maximal flexion of living subjects using a combined dual fluoroscopic imaging system (DFIS) and MRI technique (Jensen, 2005; Li et al., 2004b). The excursions of the knee motion were also analyzed in 3 flexion ranges: low flexion (<30°); middle range flexion (30° to 120°); and high range flexion (>120°). The hypothesis was that the knee had different kinematic features along the flexion path.

2. Materials and methods

Eight knees from seven healthy subjects (age, 23–49; 5 males and 2 females; BMI, 19.9–29.3 kg/m^2) with no history of knee injuries or chronic knee pain were recruited. Each subject signed a consent form approved by our institutional review board. Each knee was imaged using a 3.0T MRI scanner (Siemens, Malvern, PA) with a fat suppressed 3D spoiled gradient recalled sequence. Sagittal images with a 1 mm thickness were captured in a 180 mm × 180 mm field of view and a resolution of 512×512 pixels. These images were used to create a 3D anatomical model of the knee (including bony surfaces of the femur and tibia and their articular cartilage surfaces) in a solid modeling software (Rhinoceros©, Robert McNeel & Assoc., Seattle, WA) (DeFrate et al., 2004a).

After MR scanning, each subject performed a quasi-static single-legged lunge from full extension to maximal flexion in the field view of the two orthogonally positioned fluoroscopes (BV Pulsera; Philips, Bothell, WA). Full extension was defined as the flexion angle of the knee when the subject was standing naturally on one leg with the knee held as straight as possible. The subjects were instructed to hold the knee position for a second while bearing the body weight at each selected flexion angle (~ every 15° from full extension to maximal flexion) and allowed to use the contralateral leg and a handrail to keep their body stable if necessary (Fig. 1a). Flexion angles of the knee were monitored using a goniometer. The orthogonal fluoroscopic images and the 3D bony models of the femur and tibia were imported into a virtual space that replicated the dual fluoroscopic image system in the solid modeling software (Fig. 1b) (DeFrate et al., 2004a; Li et al., 2004a). The outline of each bone was extracted from the fluoroscopic images. The projections of the 3D femur and tibia models were matched to their corresponding outlines on the fluoroscopic images to reproduce the 3D positions of the model in space. The relative positions of the femur and tibia models were used to represent the 6DOF tibiofemoral position at each tested flexion angle (Fig. 1c). To describe the 6DOF tibiofemoral motion at a flexion angle of the knee, the coordinate systems of femur and tibia were established based on the transepicondylar axis of the femur and the bony geometry of the MR model (Van de Velde et al., 2010).

After reproducing the knee joint motion, the relative positions of the 3D surfaces of the cartilage on the femur and tibia were determined (DeFrate et al., 2004a; Li et al., 2005). The overlap of the 2 cartilage surfaces was used to represent the tibiofemoral cartilage contact. The centroid of the contact area was defined as the contact point. To quantify the motion of the contact point on the tibia, the contact points were projected on the plane defined by the anterior-posterior (AP) and medial-lateral (ML) axes on the tibia plateau. The anterior and medial directions were defined as positive. The values of the contact point positions were normalized to the AP and ML dimensions of the tibial plateau.

The locations of the contact points on the cartilage surfaces of the femoral condyles were quantified by 2 angles: one in the sagittal plane and the other in the transverse plane (Jensen, 2005). Firstly, a circle was fit to the posterior portion of each condyle in the sagittal plane (Fig. 2a). A line was drawn from the center of the circle to the contact point and was defined as the contact line. The contact line was then projected onto the sagittal plane. A vertical reference line was defined by drawing a radius through the center of the circle, parallel to the long axis of the femur. The angle between the sagittal plane projection of the contact line and the vertical reference line was defined as the *sagittal plane contact angle* (α). To define the deviation angle (β), a circle in the transverse plane was fitted to the condyles in the plane containing the contact line, perpendicular to the sagittal plane. To define zero deviation, a line was then drawn from the center of the circle to the joint line (the line tangent to both condyles). The deviation angle was then measured by calculating the angle between the projections of the contact line and the reference on the transverse plane (Fig. 2b).

A one-way analysis of variance (ANOVA) and a post hoc Student Newman-Keuls test were used to detect statistically significant differences in the 6DOF motion of the tibiofemoral joint in different ranges of knee flexion angle. Independent variable was the range of flexion angle (low flexion range; i.e., full extension to 30° of flexion; middle flexion range; i.e., 30° to 120° of flexion; and high flexion range; i.e., 120° to maximal flexion). The dependent variables were defined as changes in the anteroposterior and mediolateral translations, internal/external rotation and varus/valgus rotation within each range of knee flexion. Also, a two-way repeated measures ANOVA and a post hoc Student Newman-Keuls test were used to analyze the positions of contact points on the tibial and femoral articular cartilage surfaces. The range of knee flexion angles (low, middle, and high) and the knee

compartments (medial and lateral) were considered as independent variables. Level of significance was set at p<0.05.

3. Results

3.1. 6DOF knee kinematics during high flexion

The flexion angles ranged from full extension of $-2.9° \pm 7.0°$ to the maximal flexion of $145.3° \pm 5.7°$ during the quasi-static single-legged lunge of this subject group (Fig. 3 and Table 1). At every 15° of knee flexion, the kinematics of the knee joint was compared with those of the initial position (the knee position during the MRI scanning) as shown in Figure 3. From full extension to 30° flexion of the knee, the femur moved posteriorly 4.4 ± 3.1 mm; from 30° to 120°, the femur moved 13.3 ± 3.2 mm posteriorly, and from 120° to maximal flexion, the femur moved 7.5 ± 4.3 mm posteriorly (Fig. 3a). Posterior femoral excursion in the middle flexion range was significantly larger than those of low and high flexion ranges. In the medial-lateral direction, the femur moved laterally 1.7 ± 1.1 mm from full extension to 30° of flexion, 0.1 ± 1.7 mm laterally from 30° to 120° of flexion, and 3.8 ± 2.6 mm medially from 120° to maximal flexion (Fig. 3b). Femoral excursion in medial-lateral direction at high range of flexion was significantly greater compared to that of low and middle flexion ranges.

The tibia rotated internally by $6.1° \pm 7.6°$ (Fig. 3c) and in varus by $1.7° \pm 2.6°$ from full extension to 30° of flexion (Table 1). From 30° to 120°, the tibia rotated internally by $2.1° \pm 8.2°$ and in varus by $4.1° \pm 3.6°$. From 120° to maximal flexion, the tibia internally rotated by $7° \pm 6.2°$ and in valgus by $0.2° \pm 3.3°$.

3.2. Articular contact tracking on tibial plateau and femoral condyles

In anteroposterior direction, the contact points sharply moved posteriorly both in the medial and lateral compartments from full extension to 30° of knee flexion by 5.1 ± 4.9 mm and 4.9 ± 3.9 mm, respectively (Fig. 4, Table 1). Thereafter, the contact points slightly moved posteriorly by 4.2 ± 1.6 mm in the medial compartment and 5.0 ± 2.9 mm in the lateral compartment from 30° to 120° of flexion. From 120° flexion to maximal flexion, the medial contact point moved 1.9 ± 2.1 mm posteriorly and the lateral contact point moved 4.8 ± 2 mm posteriorly (P< 0.05).

The tibiofemoral articular contact points are shown in Figure 5 on both medial and lateral femoral condyles from full extension to maximal knee flexion. The contact angles consistently increased both on the medial and lateral femoral condyles from full extension to the maximal knee flexion (Fig. 6a, Table 2) and reached posterior-proximal tip portion of the femoral condyles. In general, the contact angles from 30° to 120° were larger than those at the low and high flexion ranges. The deviation angle of the contact point on the lateral femoral condyle slightly decreased from $12.5° \pm 3.5°$ (120° of flexion) to $10.5° \pm 3.8°$ (maximal flexion) at high flexion of the knee (Fig. 6b, Table 2). Lateral femoral condyle lift at maximal flexion was observed in 3 knees.

4. Discussion

This study presented in vivo 6DOF kinematics of the knee and the articular cartilage contact patterns during a quasi-static single-legged lunge from full extension to maximal flexion. The data indicated that the internal tibial rotation increased sharply at low flexion angles, maintained a small variation in the middle range of flexion, and sharply increased again at high flexion angles. A high varus rotation was only observed at high flexion angles. Contact points on the medial compartment slightly moved posteriorly more than those on the lateral compartment at the low flexion range, but moved similarly compared to those on the lateral

compartment at the middle range of flexion. At high flexion range, the contact point moved less on the medial compartment compared to the lateral compartment. The data supported our hypothesis, indicating that the knee motion cannot be described using one character in the entire range of flexion.

A sharp increase in internal tibial rotation with flexion in low flexion angles has been reported in numerous knee kinematics studies (Hill et al., 2000; Li et al., 2004b; Moro-oka et al., 2008; Tanifuji et al., 2011). Many studies also reported a continuously internal tibial rotation at middle range of knee flexion (Asano et al., 2001; Moro-oka et al., 2008). However, this study revealed a relative constant level of tibial rotation in the middle range of flexion, that is similar to the observations obtained using an in-vitro robotic test of cadaveric knees under simulated muscle loads (Conditt et al., 2004). At the maximal flexion range, several studies have reported a continued internal tibial rotation with flexion (Moro-oka et al., 2008; Nakagawa et al., 2000; Yildirim et al., 2007), similarly to the current study.

Many studies reported that during knee flexion, the translation of the femoral condyle with respect to tibial plateau is slightly towards posterior on medial side, whereas the lateral femoral condyle translated consistently in the posterior direction (Fukagawa et al., 2010; Johal et al., 2005; Tanifuji et al., 2011). This type of knee motion behavior has been referred to as a medial-pivoting rotation of the knee (Hill et al., 2000; Jensen, 2005; Johal et al., 2005; Tanifuji et al., 2011), where the knee axially rotates with respect to an axis located on the medial side of the knee during flexion (Johal et al., 2005; Tanifuji et al., 2011), Hill and Johal investigated the kinematics of the knee using open-MRI and Tanifuji used single-plane fluoroscopy during squatting. However, during gait and running cycle, the knee was shown to rotate with respect to an axis that is located on the lateral side of the knee (Dyrby and Andriacchi, 2004; Hoshino and Tashman, 2012; Koo and Andriacchi, 2008; Kozanek et al., 2009), where Dyrby and Koo measured the kinematics of the knee during walking or leg extension using the motion analysis, Hoshino investigated the kinematics of the knee during running using CT 3D model and dynamic stereo X-ray system and Kozanek studied the kinematics of the knee during walking using the MRI 3D model and the dual fluoroscopy imaging system. These studies on various weight-bearing functions of the knee reported various patterns of the medial and lateral femoral condyle translations, which do not support the medial-pivoting description of the knee flexion (Fukagawa et al., 2010; Johal et al., 2005; Tanifuji et al., 2011). Instead, these data indicated that the kinematics is not uniform along the knee flexion path, especially during higher flexion, indicating that the knee kinematics is activity (or loading) dependent.

It should be noted that the posterior femoral condyle translation has been described using various definitions in literature. For example, Most et al. defined the femoral condyles along the transepicondylar line (Most et al., 2004); Tanifuji et al. described the femoral condyles using the geometric center line (Tanifuji et al., 2011); many directly measured the tibiofemoral translations using the motion of the articular contact points (DeFrate et al., 2004b; Fukagawa et al., 2010; Hill et al., 2000; Nakagawa et al., 2000), where Defrate et al (DeFrate et al., 2004b) measured tibiofemoral contact kinematics using the direct cartilage contact using MRI 3D model and dual fluoroscopy during weight-bearing single-legged lunge and Dennis et al. (Dennis et al., 2005) using the closest locations between the tibial and femoral boney surfaces with the CT 3D model and single plane fluoroscopy during weight-bearing deep knee bend. In current study, both the transepicondylar line and the tibiofemoral cartilage contact were used to describe the femoral condyles motions from full extension to maximal flexion of the knee. Different definitions of the motion axes among the various studies might lead to different values of the knee joint kinematics data, but the trend of the tibiofemoral motion was similar among these studies.

The lateral femoral condyle lift at maximal flexion was observed in three knees. The medial femoral shaft was close to the posterior edge of the tibial plateau at high flexion angles. The soft tissue was compressed between the tibial and femoral shafts that might serve as a pivot point for motion of the knee in high flexion (Conditt et al., 2004). Yildirim et al. (Yildirim et al., 2007) reported that at 155° of flexion, the contacts on the femur were at the extreme superior-posterior region of the articular surfaces using a cadaveric testing model. On the medial side, there was also contact between the posterior femoral cortex and the posterior edge of the tibia, which represented an "impingement" of the knee, but this did not occur laterally. Zelle et al. (Zelle et al., 2009) found that at the maximal flexion (155°), the compressive force of the knee decreased from 4.89 to 2.90 times of the bodyweight in case where a thigh-calf contact was included. There was a correlation between a subject's thigh and calf circumference and the force reduction at maximal flexion due to thigh-calf contact (Zelle et al., 2009). These data indicated that the posterior impingement between bone and soft tissue may play an important role in the stability of the knee in high flexion. Future studies should examine the extent of compression at the medial and lateral sides of the knee at in-vivo high flexion angles of the knee.

Many of the knee kinematics during flexion were measured under non-weightbearing conditions or with partial loads (Hill et al., 2000; Johal et al., 2005; Nakagawa et al., 2000). The loading conditions of the knee among these studies are different from those of the knee during a squatting (Johal et al., 2005; Tanifuji et al., 2011), a single-legged lunge (Moro-oka et al., 2008), or stair ascending (Moro-oka et al., 2008), etc. In addition, the full extension position was also inconsistent among the various studies. For example, the full extension during supine, passive condition may not be the same as the full extension position during a full body weight-bearing single-legged standing. Even in similar single-legged flexion, current study measured higher medial tibiofemoral cartilage contact translation than those reported previously (Dennis et al., 2005; Li et al., 2005). A longer holding time at each knee flexion angle in Li et al., 2005 study (4 seconds, compared to 1 second in the current study) could cause different cartilage deformation (Hosseini et al., 2010) and consequently a different medial tibiofemoral cartilage contact translation. Therefore, kinematics data of the knee should be explained only relevant to the loading conditions during the kinematics measurement. A careful description of the full extension of the knee is important in reporting the kinematics data of the knee.

It should be noted that this study was based on the in vivo weight-bearing quasistatic single-legged lunge. Future studies should investigate the kinematics and articular cartilage contact during dynamic flexion-extension cycle of the knee as the knee motion is loading-dependent. The ground reaction forces were not measured in this study. Body mass may affect knee kinematics in high flexion. Therefore, it is interesting to investigate the effect of body mass index on the high flexion of the knee. Sex may also have an influence on knee kinematics in high flexion (Zeller et al., 2003). It is warranted to recruit more subjects in future to analyze the sex effect on knee kinematics in high flexion angles. Menisci were not modeled in this study since the fluoroscopy technique could not determine the meniscus motion. Therefore, the contact kinematics should be explained as the cartilage-to-cartilage contact only. Despite these limitations, this study clearly indicated the path dependence of the knee motion characters during a high flexion of the knee.

In conclusion, this study quantitatively described the motion characteristics of the knee during a quasi-static weight-bearing single-legged lunge from full extension to maximal flexion of the knee. The tibiofemoral articular cartilage contact points were measured on both tibial and femoral cartilage surfaces. The data in this study revealed that the overall excursions of the articular contact points were similar in the medial and lateral compartments. On average, the excursion at medial side is higher in the low flexion range,

similar in the middle flexion range and smaller at the high flexion range when compared to those at the lateral side. The locations of the tibiofemoral articular cartilage contact points were in the central portion of the medial compartment and in the posterior half of the lateral compartment. These data may provide important insights for further improvement of contemporary TKA surgeries in order to achieve physical high flexion activities.

Acknowledgments

References

Acker SM, Cockburn RA, Krevolin J, Li RM, Tarabichi S, Wyss UP. Knee kinematics of high-flexion activities of daily living performed by male Muslims in the Middle East. J Arthroplasty. 2011; 26:319–327. [PubMed: 21036011]

Amin S, Goggins J, Niu J, Guermazi A, Grigoryan M, Hunter DJ, Genant HK, Felson DT. Occupation-related squatting, kneeling, and heavy lifting and the knee joint: a magnetic resonance imaging-based study in men. J Rheumatol. 2008; 35:1645–1649. [PubMed: 18597397]

Anderst WJ, Tashman S. A method to estimate in vivo dynamic articular surface interaction. J Biomech. 2003; 36:1291–1299. [PubMed: 12893037]

Asano T, Akagi M, Tanaka K, Tamura J, Nakamura T. In vivo three-dimensional knee kinematics using a biplanar image-matching technique. Clin Orthop Relat Res. 2001:157–166. [PubMed: 11451115]

Conditt MA, Noble PC, Bertolusso R, Woody J, Parsley BS. The PCL significantly affects the functional outcome of total knee arthroplasty. The Journal of arthroplasty. 2004; 19:107–112. [PubMed: 15457428]

DeFrate LE, Gill TJ, Li G. In vivo function of the posterior cruciate ligament during weightbearing knee flexion. Am J Sports Med. 2004a; 32:1923–1928. [PubMed: 15572322]

DeFrate LE, Sun H, Gill TJ, Rubash HE, Li G. In vivo tibiofemoral contact analysis using 3D MRI-based knee models. J Biomech. 2004b; 37:1499–1504. [PubMed: 15336924]

Dennis DA, Mahfouz MR, Komistek RD, Hoff W. In vivo determination of normal and anterior cruciate ligament-deficient knee kinematics. J Biomech. 2005; 38:241–253. [PubMed: 15598450]

Dyrby CO, Andriacchi TP. Secondary motions of the knee during weight bearing and non-weight bearing activities. J Orthop Res. 2004; 22:794–800. [PubMed: 15183436]

Fitz W, Sodha S, Reichmann W, Minas T. Does a modified gap-balancing technique result in medial-pivot knee kinematics in cruciate-retaining total knee arthroplasty? A pilot study. Clin Orthop Relat Res. 2012; 470:91–98. [PubMed: 21984353]

Fukagawa S, Matsuda S, Tashiro Y, Hashizume M, Iwamoto Y. Posterior displacement of the tibia increases in deep flexion of the knee. Clin Orthop Relat Res. 2010; 468:1107–1114. [PubMed: 19847583]

Gao B, Zheng NN. Investigation of soft tissue movement during level walking: translations and rotations of skin markers. Journal of biomechanics. 2008; 41:3189–3195. [PubMed: 18930462]

Hill PF, Vedi V, Williams A, Iwaki H, Pinskerova V, Freeman MA. Tibiofemoral movement 2: the loaded and unloaded living knee studied by MRI. J Bone Joint Surg Br. 2000; 82:1196–1198. [PubMed: 11132286]

Hoshino Y, Tashman S. Internal tibial rotation during in vivo, dynamic activity induces greater sliding of tibio-femoral joint contact on the medial compartment. Knee Surg Sports Traumatol Arthrosc. 2012; 20:1268–1275. [PubMed: 22041716]

Hosseini A, Van de Velde SK, Kozanek M, Gill TJ, Grodzinsky AJ, Rubash HE, Li G. In-vivo time-dependent articular cartilage contact behavior of the tibiofemoral joint. Osteoarthritis and cartilage / OARS, Osteoarthritis Research Society. 2010; 18:909–916.

Jensen LK. Knee-straining work activities, self-reported knee disorders and radiographically determined knee osteoarthritis. Scand J Work Environ Health. 2005; 31(Suppl 2):68–74. [PubMed: 16363449]

Johal P, Williams A, Wragg P, Hunt D, Gedroyc W. Tibio-femoral movement in the living knee. A study of weight bearing and non-weight bearing knee kinematics using 'interventional' MRI. J Biomech. 2005; 38:269–276. [PubMed: 15598453]

Koo S, Andriacchi TP. The knee joint center of rotation is predominantly on the lateral side during normal walking. J Biomech. 2008; 41:1269–1273. [PubMed: 18313060]

Koo S, Rylander JH, Andriacchi TP. Knee joint kinematics during walking influences the spatial cartilage thickness distribution in the knee. J Biomech. 2011; 44:1405–1409. [PubMed: 21371712]

Kozanek M, Hosseini A, Liu F, Van de Velde SK, Gill TJ, Rubash HE, Li G. Tibiofemoral kinematics and condylar motion during the stance phase of gait. J Biomech. 2009; 42:1877–1884. [PubMed: 19497573]

Kuroyanagi Y, Mu S, Hamai S, Robb WJ, Banks SA. In vivo knee kinematics during stair and deep flexion activities in patients with bicruciate substituting total knee arthroplasty. J Arthroplasty. 2012; 27:122–128. [PubMed: 21507605]

Li G, DeFrate LE, Park SE, Gill TJ, Rubash HE. In vivo articular cartilage contact kinematics of the knee: an investigation using dual-orthogonal fluoroscopy and magnetic resonance image-based computer models. The American journal of sports medicine. 2005; 33:102–107. [PubMed: 15611005]

Li G, DeFrate LE, Sun H, Gill TJ. In vivo elongation of the anterior cruciate ligament and posterior cruciate ligament during knee flexion. The American journal of sports medicine. 2004a; 32:1415–1420. [PubMed: 15310565]

Li G, Wuerz TH, DeFrate LE. Feasibility of using orthogonal fluoroscopic images to measure in vivo joint kinematics. J Biomech Eng. 2004b; 126:314–318. [PubMed: 15179865]

Moro-oka TA, Hamai S, Miura H, Shimoto T, Higaki H, Fregly BJ, Iwamoto Y, Banks SA. Dynamic activity dependence of in vivo normal knee kinematics. J Orthop Res. 2008; 26:428–434. [PubMed: 17985389]

Most E, Axe J, Rubash H, Li G. Sensitivity of the knee joint kinematics calculation to selection of flexion axes. J Biomech. 2004; 37:1743–1748. [PubMed: 15388317]

Moynihan AL, Varadarajan KM, Hanson GR, Park SE, Nha KW, Suggs JF, Johnson T, Li G. In vivo knee kinematics during high flexion after a posterior-substituting total knee arthroplasty. Int Orthop. 2010; 34:497–503. [PubMed: 19387643]

Nakagawa S, Kadoya Y, Todo S, Kobayashi A, Sakamoto H, Freeman MA, Yamano Y. Tibiofemoral movement 3: full flexion in the living knee studied by MRI. J Bone Joint Surg Br. 2000; 82:1199–1200. [PubMed: 11132287]

Palmer KT. Occupational activities and osteoarthritis of the knee. Br Med Bull. 2012; 102:147–170. [PubMed: 22544778]

Tamaki M, Tomita T, Watanabe T, Yamazaki T, Yoshikawa H, Sugamoto K. In vivo kinematic analysis of a high-flexion, posterior-stabilized, mobile-bearing knee prosthesis in deep knee bending motion. J Arthroplasty. 2009; 24:972–978. [PubMed: 19033084]

Tanifuji O, Sato T, Kobayashi K, Mochizuki T, Koga Y, Yamagiwa H, Omori G, Endo N. Three-dimensional in vivo motion analysis of normal knees using single-plane fluoroscopy. J Orthop Sci. 2011; 16:710–718. [PubMed: 21892788]

Van de Velde SK, Hosseini A, Kozanek M, Gill TJ, Rubash HE, Li G. Application guidelines for dynamic knee joint analysis with a dual fluoroscopic imaging system. Acta orthopaedica Belgica. 2010; 76:107–113. [PubMed: 20306974]

Yildirim G, Walker PS, Sussman-Fort J, Aggarwal G, White B, Klein GR. The contact locations in the knee during high flexion. Knee. 2007; 14:379–384. [PubMed: 17683941]

Zelle J, Barink M, De Waal Malefijt M, Verdonschot N. Thigh-calf contact: does it affect the loading of the knee in the high-flexion range? J Biomech. 2009; 42:587–593. [PubMed: 19200996]

Zeller BL, McCrory JL, Kibler WB, Uhl TL. Differences in kinematics and electromyographic activity between men and women during the single-legged squat. The American journal of sports medicine. 2003; 31:449–456. [PubMed: 12750142]
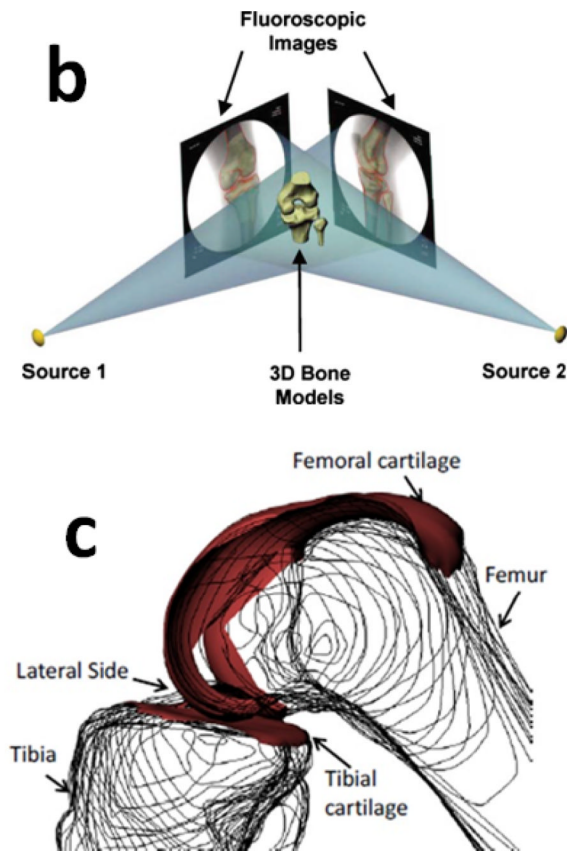
Figure 1.
(a) Subject performing a quasi-static single-legged lunge (right knee) in the DFIS. (b) Reproduction of the kinematics of the knee in a virtual DFIS. (c) Knee position at high flexion of one subject recreated in the virtual environment.
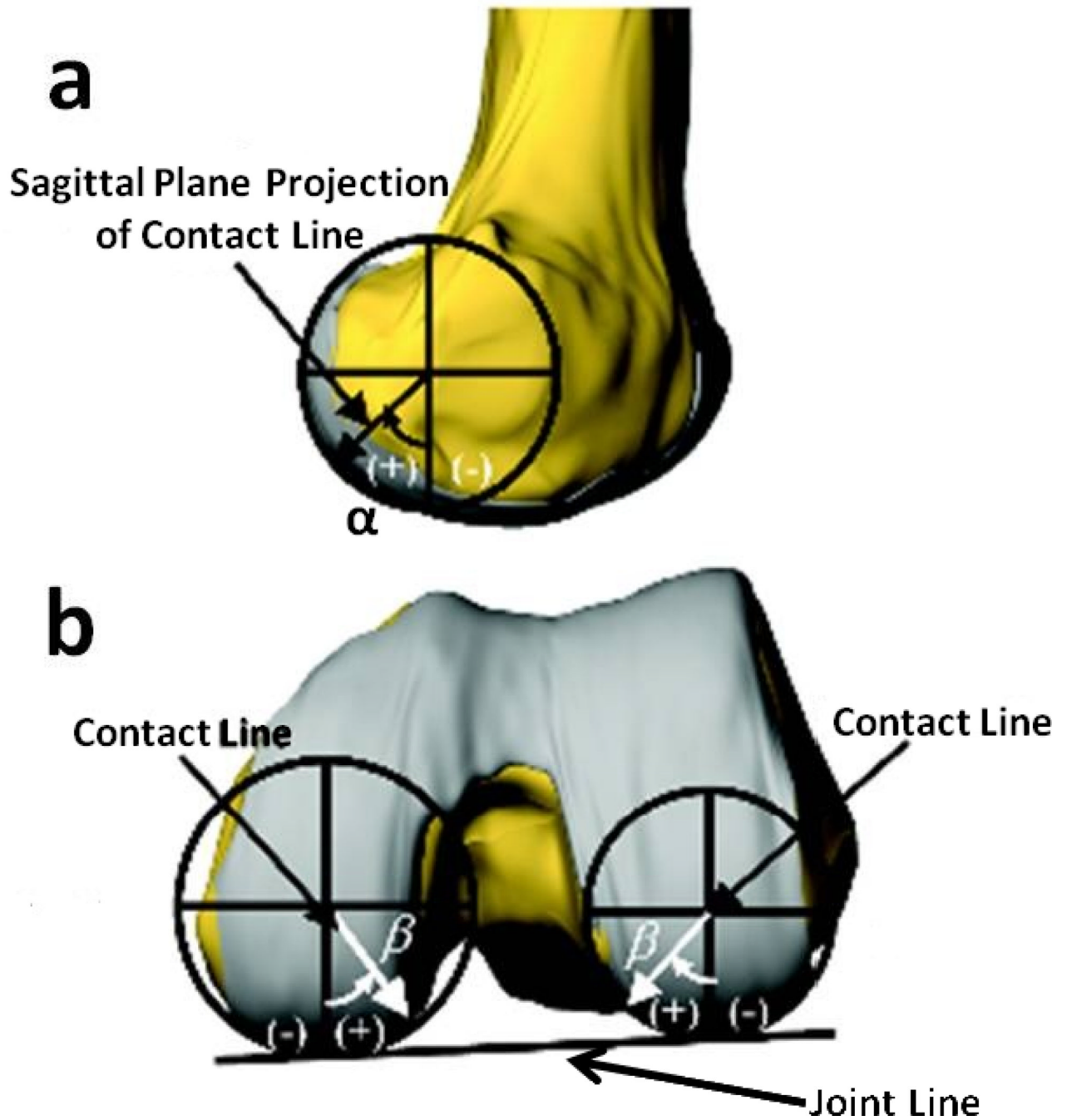
Figure 2.
A 3-dimensional knee model for a typical specimen and the definition of the coordinates used to measure the location of the contact points on the femoral condyles. (a) Definition of sagittal plane contact angle-α; (b) definition of the deviation angle-β.
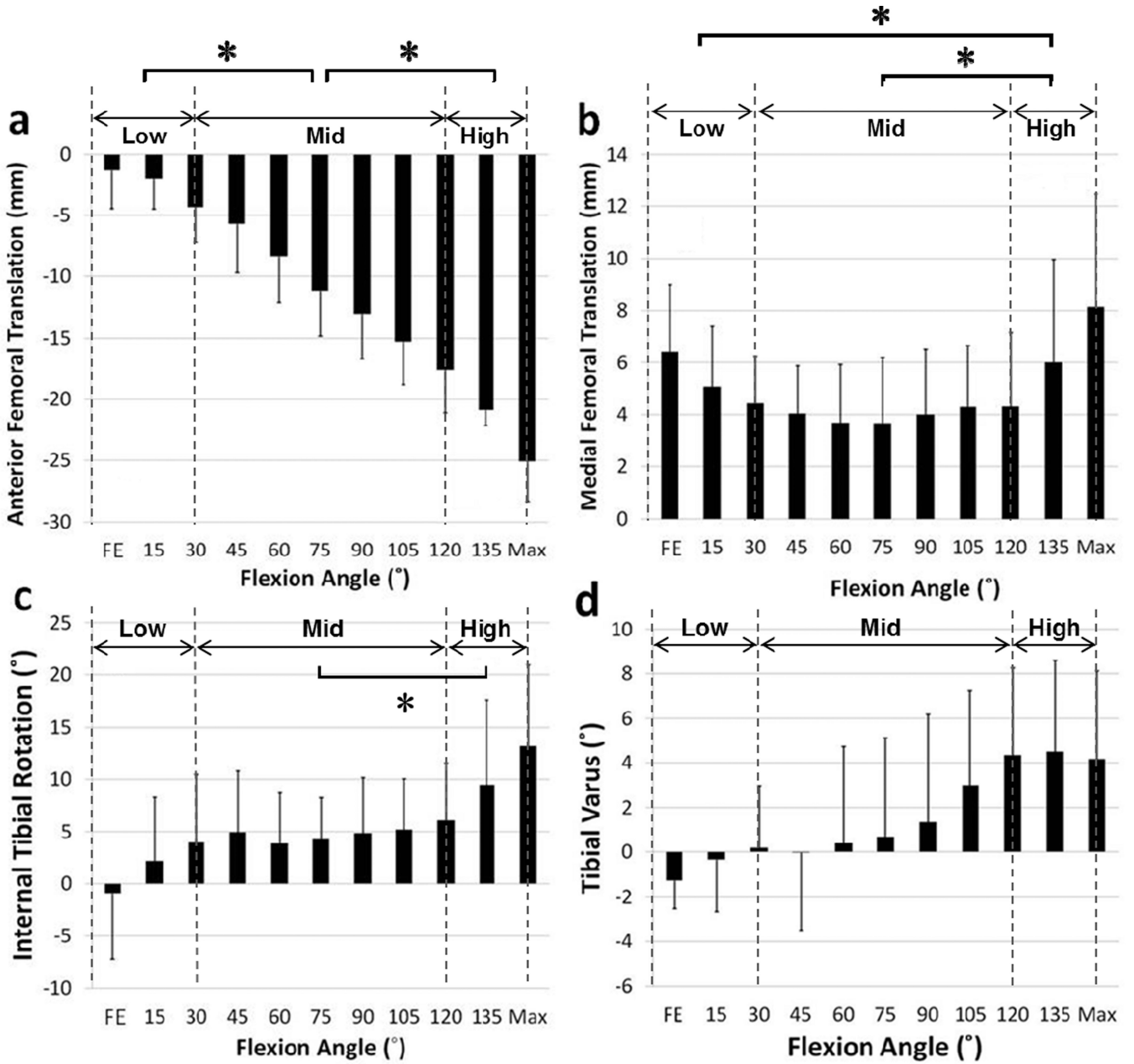
Figure 3.
(a) Anterior and (b) medial translations; (c) internal and (d) varus rotations of the tibia relative to femur during the full range of knee flexion (FE: Full extension; Max: Maximal flexion). Asterisk means a statistically significant difference in mean values between 120° and maximal flexion. The data are presented in mean values and their corresponding standard deviations.
Low: low flexion range (full extension to 30° of flexion);
Mid: middle flexion range (30° to 120° of flexion);
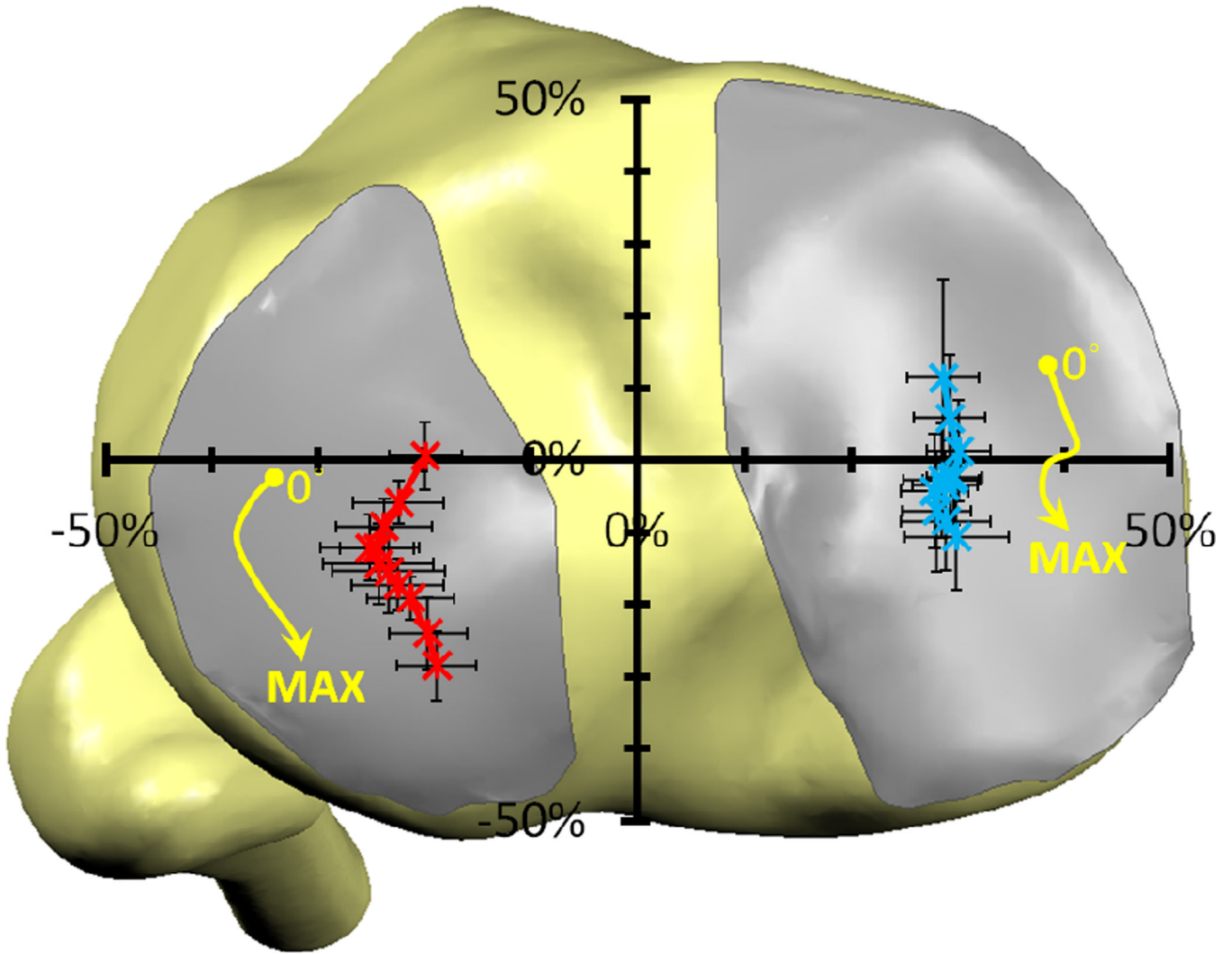High: high flexion range (120° to maximal flexion)

Figure 4.
Tibiofemoral cartilage contact positions on the medial and lateral tibial plateau at different flexion during in-vivo weight-bearing lunge. The crosses stand for the mean locations of cartilage contacts during the knee flexion and the error bars are the standard deviation.
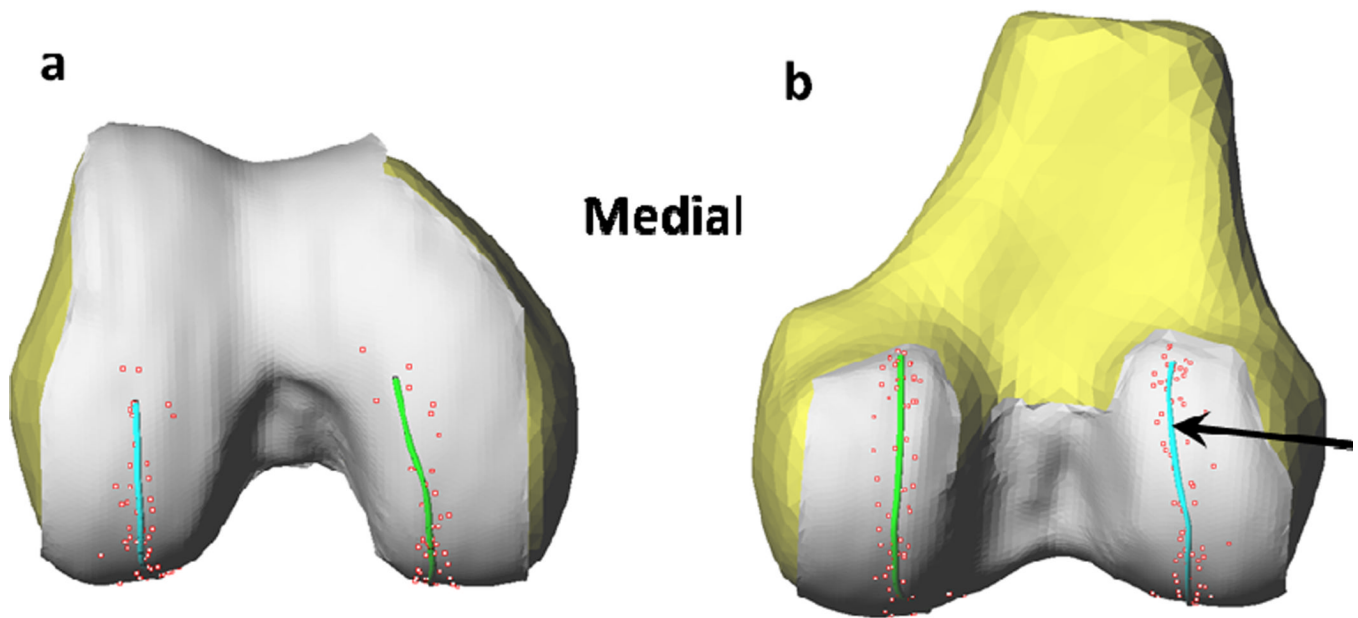
Figure 5.
Tibiofemoral cartilage contact points on the femoral condyles at different flexion angles during in-vivo weightbearing lunge. The dots on the cartilage stand for the individual contact points of all the subjects and the lines (arrow) shows the average location of the contact. (a) Distal view; (b) posterior view.
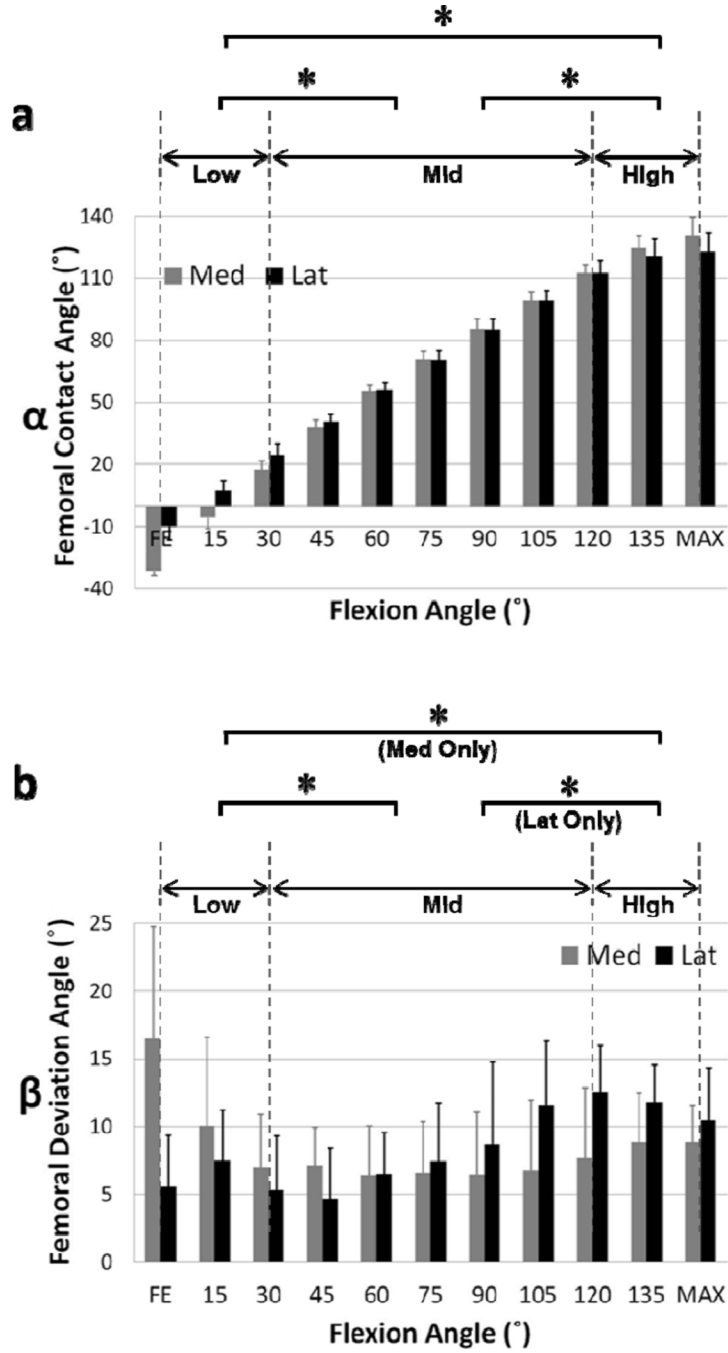
Figure 6.
(a) Tibiofemoral cartilage contact angles and (b) deviation angles on the medial and lateral femoral condyles. The columns stand for the mean angles and the error bars are standard deviations. (FE: Full extension; Max: Maximal flexion)

Table 1

Femoral translation, tibial rotation and tibiofemoral contact kinematics in different flexion ranges of the Knee (Mean ± SD)

Motions	FE–30°	30°–120°	120°–MaxF	FE–MaxF
Femoral Anterior Translation (mm)	−4.4±3.1	−13.3±3.2[*]	−7.5±4.3[†]	−25.2±5.0
Femoral Medial Translation (mm)	−1.7±1.1	−0.1±1.7	3.8±2.6[*†]	2.0±3.4
Tibial Internal Rotation (°)	6.1±7.6	2.1±8.2	7.0±6.2	15.2±9.2
Tibial Varus (°)	1.7±2.6	4.1±3.6	−0.2±3.3[†]	5.6±4.9
Medial A-P Contact (mm)	−5.1±4.9	−4.2±1.6	−1.9±2.1	−11.1±3.3
Lateral A-P Contact (mm)	−4.9±3.9	−5.0±2.9	−4.8±2.0[**]	−14.6±3.7[**]

FE: Full extension; MaxF: Maximal flexion.

Positive values indicate internal rotation, varus, and anterior and medial translation, whereas negative values indicate external rotation, valgus, and posterior and lateral translation.

[*] Significant difference between the range and the FE–30° of flexion angles;

[†] Significant difference between the range and the 30°–120° of flexion angles;

[**] Significant difference between the medial and lateral A-P contact positions.

Table 2

Articular contact angles on the femoral condyles in different flexion ranges of the knee (Mean ± SD)

	FE–30°	30°–120°	120°–MaxF°	FE–MaxF
Medial Femoral Contact Angle (°)	49.4±10.8	95.2±4.1[*]	18.4±5.4[*†]	162.9±12.9[‡]
Lateral Femoral Contact Angle (°)	37.9±6.2	87.8±6.7[*]	10.3±7.6[*†]	135.9±9,3
Medial Femoral Deviation Angle (°)	−7.9±7.2	0.7±5.5[*]	1.2±5.9[*]	−6.0±10.2
Lateral Femoral Deviation Angle (°)	−1.0±8.9	7.2±5.6[*]	−2.0±6.7[†]	4.1±7.2

FE: Full extension; MaxF: Maximal flexion.

[*] Significant difference with that of FE–30;

[†] Significant difference with that of 30°–120°;

[‡] Significant difference between the medial and lateral femoral contact angles.